Active zone of growing clusters: Diffusion-limited aggregation and the Eden model in two and three dimensions

Zoltán Rácz* and Michael Plischke
Physics Department, Simon Fraser University, Burnaby, British Columbia, Canada V5A 1S6
(Received 7 August 1984)

Our previous studies of the growing interface of two-dimensional clusters produced by the Eden process and by diffusion-limited aggregation are expanded and extended to $d=3$ dimension. Growth is described in terms of the motion of an active zone defined as the region of the clusters where the probability of collecting new particles is nonzero. If the description is limited to spherically averaged properties then this active region can be characterized by the probability $P(r,N)dr$ that the Nth particle is deposited a distance r from the center of mass of the existing cluster. As in our previous Monte Carlo simulations of the $d=2$ case, we find that, for large N, $P(r,N)=(\sqrt{2\pi}\xi_N)^{-1}\exp[-(r-\bar{r}_N)^2/2\xi_N^2]$ with $\bar{r}_N\sim N^{\nu}\sim N^{1/D}$, where D is the fractal dimension of the infinite cluster and $\xi_N\sim N^{\bar{\nu}}$ where $\bar{\nu}<\nu$, indicating the presence of a second diverging length in these growth processes. We also study the center-of-mass motion of growing clusters. We find that one has to be especially careful with simulations of diffusion-limited aggregation because discarding particles which wander too far away from the cluster generates an effective force on the center of mass, resulting in a motion which can obscure the intrinsic structure of the clusters.

I. INTRODUCTION

A number of nonequilibrium phenomena have been described in terms of models in which a single cluster grows through the addition of individual particles.[1] The two elementary growth processes, of which a number of variants have been proposed, are diffusion-limited aggregation[2] (DLA) and the Eden process.[3] The DLA process and its generalizations[4,5] seem to describe particularly well the aggregation of smoke particles,[6] colloid aggregation,[7] electric breakdown,[8] and some limits of two-fluid displacement in porous media,[9] while the Eden model might be useful in characterizing the growth of tumors,[3] and its variants[10,11] may contain some of the important features of crystal growth.[12]

The study of these growth models has to this point been concentrated mainly on the properties of the final state of the cluster, i.e., on the structure in a region of space where no further particles accumulate. These frozen structures are indeed fascinating. Diffusion-limited aggregation and variants of the basic model,[4,5,13–15] as well as invasion percolation processes,[16,17] lead to frozen structures which are scale invariant with a fractal dimension $D<d$ where d is the Euclidean dimension of the space in which the process takes place. Growth seems to result in clusters which possess structure on every length scale even in some cases[18–21] where $D=d$. The numerical values of the fractal dimension D in different growth models have been accurately determined through simulations. At the moment, however, no satisfactory analytic theory exists for the calculation of D although a number of mean-field-type approximations have been developed[22–26] which yield reasonable numerical values for D and a simple position-space renormalization group procedure has also been proposed.[27]

We believe that a proper theory for the frozen structure can only be constructed after understanding the surface properties of growing clusters. The cluster is built in an "active" zone, which is usually the outer part of the surface collecting all the new particles in a given stage of the growth. Since the frozen bulk and the dynamics of the process are related to each other only through this active zone and since our purpose is the evaluation of the bulk properties starting from the dynamical equations, clearly the principal task should be to find a way of describing the active zone and then to calculate the characteristic quantities appearing in that description.

There have been several attempts[22–26,28–31] to describe the growing interface in the DLA and in the Eden process. In Monte Carlo simulations, complicated quantities like interfacial mass[28] or the upper surface of a deposit[29] were studied. Although these quantities are easily evaluated in a numerical study, they seem to be too complex to be within the reach of analytical approaches. Simpler quantities are examined in mean-field-type theories of DLA where the surface is specified by a single characteristic length. This length, the screening length, can be interpreted as the penetration depth of the incoming particles, i.e., as the width of the active zone. In the absence of a systematic theory for the calculation of the screening length, it is usually obtained from some clearly oversimplified physical picture, the result being that this length scales as a simple power of the particle density[22–24] in the cluster. Yet another conjecture concerning this length comes from studies of clusters in percolation problems.[32] It is assumed[30] that there is only one divergent length in the system thus implying that the width of the surface region scales as the radius of the cluster. Naturally, the scaling behavior of the characteristic length associated with the surface predicted by the preceding theories is quite different and they are incompatible with each other.

In two recent short papers[33,34] and in this paper we attempt a somewhat more sophisticated characterization of the aggregation process by considering the probability $P(r,N)dr$ that the Nth particle is deposited in the shell bounded by the radii r and $r+dr$ measured from the center of mass of the $(N-1)$-particle cluster. On the basis of extensive Monte Carlo simulations of DLA and the Eden model in $d=2$ (a less detailed study of this case is presented in Refs. 33 and 34) and in $d=3$, we find that, in the large-N limit, $P(r,N)$ is given by

$$P(r,N)=\frac{1}{\sqrt{2\pi}\xi_N}\exp[-(r-\bar{r}_N)^2/2\xi_N{}^2] . \quad (1)$$

Thus the spherically averaged properties of these growing clusters seem to be fairly simple, they can be completely characterized by two parameters, the mean deposition radius $\bar{r}_N$ of the Nth particle and the width of the active zone ξ_N.

For large N, $\bar{r}_N$ exhibits power-law behavior

$$\bar{r}_N \approx r_0 N^{\nu} , \quad (2)$$

and since $\bar{r}_N$ is a measure of the expansion of the cluster as particles are added, the exponent ν is related[33,34] to the fractal dimension of the frozen structure by $D=\nu^{-1}$. Our results for D agree with previous calculations of this quantity.

The width of the active zone also displays interesting behavior. For DLA in $d=2$ and 3 it scales as

$$\xi_N \approx \xi_0 N^{\bar{\nu}} \quad (3)$$

with $\bar{\nu}<\nu$ thus indicating the presence of two distinctly diverging lengths in this process. The coexistence of two different scaling lengths in an isotropic system appears to be quite strange although it should be noted that the description of the surface of Ising clusters near the critical point also requires[35] an extra length which scales differently from the bulk correlation length. The numerical values of $\bar{\nu}$ suggest that the mean-field conjectures[22–26] regarding the screening length are quite far from reality.

For the Eden model in $d=2$ and 3, our Monte Carlo data strongly suggests that the singularity of ξ_N is of the form

$$\xi_N \approx \frac{1}{d}\ln N \quad (4)$$

which might be thought of as the $\bar{\nu}\to 0$ limit of formula (3).

The role of $\bar{\nu}$ in determining the properties of the frozen structure is not transparent but it is quite clear that it is intimately related to the dynamics of the process in question. In DLA, ξ_N is the screening length, a measure of the shielding effect which is necessary to produce the loose dendritic structure characteristic of the process. The question of how to calculate $\bar{\nu}$ and then how to relate it to D is, at this stage, unanswered.

The material in this article is arranged as follows. In Secs. II and III we discuss our simulations of DLA and the Eden model, respectively, and present evidence for formulas (1)—(4). Section IV contains a discussion of the motion of the center of mass as the cluster grows. As we shall show, separating the center-of-mass motion is important for obtaining the correct surface properties of clusters of low fractal dimensionality. Finally, in Sec. V we indicate some problems and possible directions for extending the present work.

II. MONTE CARLO SIMULATIONS OF DLA

The algorithm for DLA is quite simple and a number of simulation studies of various aspects of this process have already been presented.[2,8,13,28–30,36–41] Growth begins with a seed particle at the origin of a d-dimensional lattice (square or simple cubic in our case). Individual particles then execute an unbiased random walk in the lattice and either reach a site adjacent to the existing cluster and stop or reach a distance far enough from the seed that the probability of a return to the cluster is assumed to be negligible and is discarded. Two parameters enter into the algorithm, the radius R_i at which new particles begin their random walk and the distance R_0 at which they are discarded. The starting distance R_i is presumably irrelevant as long as R_i is greater than the maximum extent of the cluster. The ratio of $\alpha=R_0/R_i$ is usually a fixed number and in our simulations we have varied α between 2 and 5. The construction of large DLA clusters is quite time consuming and we have therefore used a device of Meakin[37] to speed up the process. If a particle reaches a distance $l_0, 2l_0, 4l_0, \ldots$, from the sphere bounding the existing cluster, the step size of the random walk is arbitrarily increased to 2,4,8, ... In our simulations we have taken l_0 to be 5, 6, and 8. As in previous simulations[37] we find that the dependence of the average deposition radius $\bar{r}_N$ or the radius of gyration $R_g(N)$ on N is quite insensitive to either α or l_0. The motion of the center of mass (see Sec. IV) and, to a lesser extent, the width of the active layer, ξ_N, do, however, depend on both of these parameters.

The calculation of the quantities of interest is carried out in the following way. Clusters are grown to a maximum size in steps of 50 particles and the positions $\mathbf{r}_i$ of the particles in the cluster are recorded. At the end of such a step, the center of mass of the cluster

$$\mathbf{r}_c(N)=\left\langle \frac{1}{N}\sum_{i=1}^{N}\mathbf{r}_i \right\rangle \quad (5)$$

is determined and the radius of gyration $R_g(N)$ is calculated as

$$R_g^2(N)=\left\langle \frac{1}{N}\sum_{i=1}^{N}[\mathbf{r}_i-\mathbf{r}_c(N)]^2 \right\rangle , \quad (6)$$

where the angular brackets denote an average over the ensemble of different clusters. Then $\bar{r}_N$ is found by averaging the deposition distance from the center of mass over the next ten particles:

$$\bar{r}_N=\left\langle \tfrac{1}{10}\sum_{i=N+1}^{N+10}|\mathbf{r}_i-\mathbf{r}_c(N)| \right\rangle . \quad (7)$$

Similarly, the screening length ξ_N is determined through such a coarse-grained average

$$\xi_N^2=\left\langle \frac{1}{10}\sum_{i=N+1}^{N+10}[\mathbf{r}_i-\mathbf{r}_c(N)]^2\right\rangle-\bar{r}_N^2 . \quad (8)$$

For large N the effect of this coarse graining is expected to be negligible. It is, of course, also possible to determine $\bar{r}_N$ and ξ_N by fitting $P(r,N)$ to Gaussian [Eq. (1)]. We have used this procedure in our previous calculations[33,34] and found identical results for $N>100$ as we do using formulas (7) and (8).

Our previous results for DLA in $d=2$ (Refs. 33 and 34) were based on 4000 clusters of 2500 particles grown with $\alpha=2$. We found $\nu=0.584\pm0.02$ and $\bar{\nu}=0.48\pm0.01$ [see Eqs. (2) and (3)]. We have since constructed a large number of small clusters (1800–2500 particles) with $\alpha=3$ and 4 and $l_0=5$, 6, and 8. Our results for these clusters confirm the values of ν and $\bar{\nu}$ reported in the earlier articles. In order to investigate possible finite-size effects we have also grown 160 clusters of 10 000 particles with $\alpha=4$ and $l_0=8$. The results are displayed in Fig. 1. The solid lines are best fits to $\bar{r}_N$, R_g, ξ_N, and $r_c(N)$ determined from smaller clusters. A number of features of Fig. 1 are noteworthy. First of all we see that the convergence of the mean values to a final functional form is rather slow. Using very small clusters ($N\leq500$) we have found that the order of 500 clusters is necessary before the fluctuations in ξ_N are reduced to the size of a point in the plot. More significant is the fact that while the points for $\bar{r}_N$ and $R_g(N)$ bracket the appropriate curves there is considerable deviation from the curve in the plot of ξ_N at large

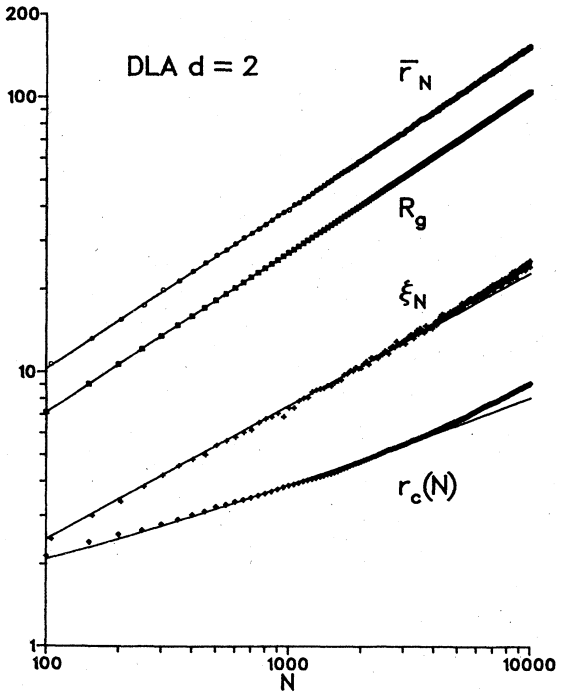

FIG. 1. Mean deposition radius $\bar{r}_N$, radius of gyration $R_g(N)$, width of the active zone ξ_N, and displacement of the center of mass $r_c(N)$ for 160 DLA clusters of 10 000 particles. The solid curves $\bar{r}_N=0.693N^{0.585}$, $R_g(N)=0.489N^{-0.582}$, $\xi_N=0.266N^{0.484}$, and $r_c(N)=0.758\pm0.242N^{0.370}$ have been determined through analysis of 4000 clusters of 2500 particles.

N. On the same graph we have also displayed a plot of the distance of the center of mass, $r_c(N)$, from the seed particle along with the curve $r_c(N)=0.242N^{\eta}+0.758$ with $\eta=0.37$ which provides the best three-parameter fit to the data for smaller clusters. One sees that for large N the center of mass deviates considerably from this curve and the deviation occurs at about the same value of N at which the upturn in ξ_N begins. Indeed, analysis of the data indicates that for the 160 samples of 10 000 particles, the best fit is $r_c(N)=0.0385N^{0.569}+1.814$. The exponent η has thus become larger than $\bar{\nu}$. For large N the drift of the center of mass is therefore more important than the intrinsic width of the active zone. A least-squares analysis of various subsets of the data in the range $50<N<N_c$ shows that all exponents (including ν to 0.594) increase for $N_c>2500$ and for $N_c=10\,000$, $\bar{\nu}\approx\eta$. We believe that this behavior is due to the finite value of α. As we show in more detail in Sec. IV, the finite distance at which the diffusing particles are discarded generates an effective force on the center of mass and this force seems to become more important as the cluster becomes larger. The distance l_0 at which the step size changes also has an effect on the behavior of the center of mass. When l_0 is decreased to 6 for fixed $\alpha=4$, the crossover to the régime $\eta\approx\nu$ occurs for lower values of N. Thus, although our results, obtained in the region $N<2500$ where no dependence on α and l_0 is observed, support the conclusion $\bar{\nu}<\nu$, to confirm this result simulations with larger values of α and l_0 will have to be carried out. Further discussion of this problem can be found in connection with the $d=3$ results below and also in the discussion of the center-of-mass motion (Sec. IV).

We turn now to the three-dimensional case. We have constructed 3000 clusters of 1010 particles using $\alpha=5$ and $l_0=8$ as well as other values of α and l_0 which we do not report on in detail. The drift of the center of mass is also important in three dimensions. The maximum lattice which can be conveniently accessed on our computer is $63\times63\times63$. Although $\bar{r}_N$ and ξ_N for $N=1500$ are 16.13 and 3.53, respectively, we have found that clusters as small as 1200 particles occasionally extend beyond the bounds of this lattice. In order to avoid any bias due to the exclusion of such clusters we restrict our analysis to the smaller clusters.

In Fig. 2 we display the function $P(r,N)$ for a number of values of N. We see that the solid curves [Eq. (1)] provide an excellent fit to the data as they do in two dimensions.[33,34] In Fig. 3 we have plotted $\bar{r}_N$, $R_g(N)$, and ξ_N as a function of N along with curves determined through the following analysis of the data. The functions $\bar{r}_N$, $R_g(N)$, and ξ_N were fitted to the form

$$y(N)=AN^{\epsilon}+B , \quad (9)$$

where y represents $\bar{r}_N$, $R_g(N)$, or ξ_N and ϵ is the appropriate exponent, ν or $\bar{\nu}$. For a given choice of ϵ, A and B are determined by a least-squares fit of (9) to the 20 equally spaced data points for $y(N)$ in the range $50\leq N\leq1000$. The values of the exponent quoted in Table I is the one for which the minimum χ^2 is obtained and the uncertainty, Δ, in ϵ is obtained from the criterion

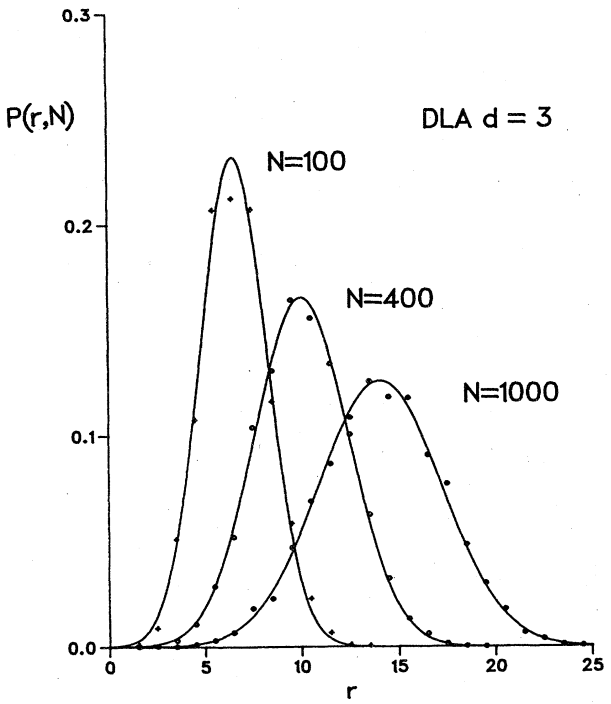

FIG. 2. Probability $P(r,N)$ that the Nth particle is deposited a distance r from the center of mass of an $N-1$ particle cluster for DLA in $d=3$. The solid lines correspond to Eq. (1) with $\bar{r}_N$ and ξ_N determined from 3000 clusters and the points determined from 1000 clusters.

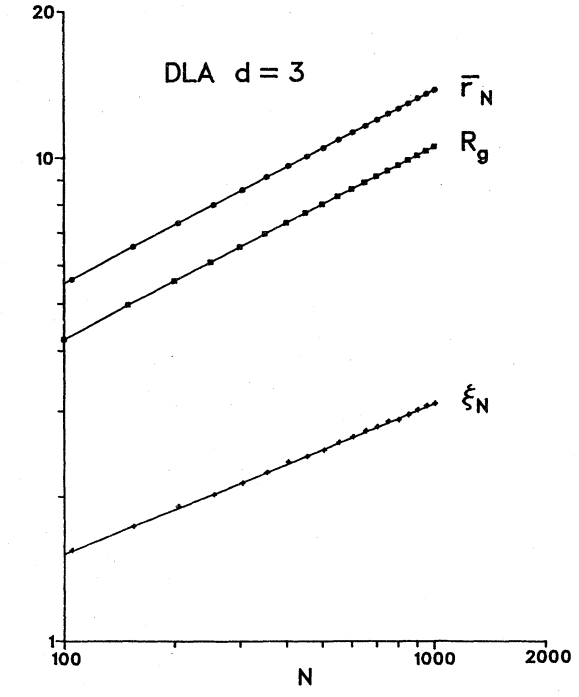

FIG. 3. Plot of $\bar{r}_N$, ξ_N, and $R_g(N)$ vs N for 3000 clusters of 1000 particles for three-dimensional DLA. Solid curves $\bar{r}_N=0.064+0.859N^{0.401}$, $R_g(N)=-0.063+0.702N^{0.393}$, and $\xi_N=0.084+0.322N^{0.324}$.

TABLE I. Results of a three-parameter fit, Eq. (9), to the data for DLA clusters in three dimensions.

	$\nu(\bar{\nu})$	A	B
$\bar{r}_N$	0.401±0.009	0.86±0.07	0.06±0.20
$R_g(N)$	0.393±0.003	0.70±0.02	−0.06±0.05
ξ_N	0.32 ±0.05	0.32±0.10	0.08±0.30

$$\chi^2(\epsilon\mp\Delta,A(\epsilon\mp\Delta),B(\epsilon\mp\Delta))-\chi^2(\epsilon,A(\epsilon),B(\epsilon))$$
$$=\chi^2(\epsilon,A(\epsilon),B(\epsilon))\ .$$

The error bars in A,B are given by $A(\epsilon\mp\Delta)-A(\epsilon)$ and $B(\epsilon\mp\Delta)-B(\epsilon)$. This uncertainty is purely statistical. There may be systematic deviations due to the finite size of the samples and the restrictive nature of the functional form (9). We mention also that a simple power law of the form $\xi_N=AN^{\bar{\nu}}$ also fits the data for ξ_N very well with $\bar{\nu}=0.31\pm0.01$ and $A=0.36\pm0.02$. For this choice of functional form the exponent $\bar{\nu}$ is within the range quoted for any subset of the data in the range $(N_c,1000)$ with $N_c\lesssim350$ and shows no tendency to increase. The result $\nu=0.401\pm0.009$ is in accord with previous estimates[36,37,40] of this quantity. The value of $\bar{\nu}=0.32\pm0.05$, however, agrees neither with mean-field conjectures[22–24] [$\bar{\nu}=\nu d-1\simeq0.2$, $\bar{\nu}=(\nu d-1)/2\approx0.1$] nor with the scaling assumption[30] $\bar{\nu}=\nu$, thus adding further weight to the conclusion that the growth of the active region is governed by an independently scaling length ξ_N which provides the screening mechanism responsible for the low fractal dimension of the aggregates.

To settle this point conclusively much larger clusters will have to be constructed in three dimensions. In two dimensions we have seen that the motion of the center of mass eventually dominates the behavior of the clusters. In three dimensions this problem may not be as severe. In two dimensions a particle, given sufficient time, will eventually reach the existing cluster.[42] Thus no choice of α is fundamentally satisfactory. In three dimensions this is not the case and one may be able to choose α large enough that the force on the center of mass becomes negligible.

We now comment briefly on other studies of the active zone of growing clusters. Meakin and Witten[28] have calculated the interfacial mass, $N_i(N)$, the number of particles which, in the limit of an infinite cluster, come in contact with the first N particles. This quantity is not easily related to the screening length ξ_N but an upper bound for it can be constructed by counting the number of particles in the active zone. Denoting the average density profile in clusters containing N particles by $\rho(r,N)$ we have the obvious inequality

$$N_i(N)\lesssim\rho(\bar{r}_N,N)\bar{r}_N^{d-1}\xi_N\sim N^{1-\nu+\bar{\nu}}\sim N^{0.9}$$

for both the $d=2$ and 3 cases. This inequality is clearly satisfied in Monte Carlo simulations[28] where $N_i(N)\sim N^{0.6}$ and $N_i(N)\sim N^{0.74}$ were found for $d=2$ and 3, respectively.

Meakin[29] has also determined the average height and the width of the upper surface of diffusion-limited deposits. He found for the $d=2$ and 3 cases that the width

grew with a somewhat smaller power of N than the average height. Under the assumption that the width of the upper surface is proportional to the width of the active zone, Meakin's results support our contention that $\bar{\nu} < \nu$. The justification of this assumption, however, is not entirely obvious.

III. MONTE CARLO SIMULATIONS OF THE EDEN PROCESS

The Eden model has been introduced[3] and used[43,44] to simulate biological growth processes. From a physicist's point of view, the significance of this model is in its implicity. Simulation studies[31,33,45] and general considerations[30,45] suggest $D=d$ for Eden clusters and, furthermore, there is evidence from simulations that the process is space filling, i.e., the particle density goes to 1 deep inside the cluster. The model is not trivial, however, since the boundary of the clusters is not sharp. As our simulations, described in this section, indicate, the width of the surface region diverges as the logarithm or as a small power of the number of particles in the cluster. Thus the model poses some challenge but, at the same time, is simple enough to hope that it can be treated analytically. Such an analytic treatment might then serve as a starting point for devising systematic methods of calculating the properties of growing clusters.

The algorithm of the Eden model is exceedingly simple and well suited for computer simulations. The process is started by placing a seed particle on a lattice site. The cluster is then grown by adding particles at randomly selected unoccupied sites adjacent to the existing cluster. In this way, we have grown 20 000 and 16 000 clusters on the square and simple-cubic lattices, respectively, with 4000 particles in each cluster.

The plots of the probability distribution functions $P(r,N)$ and the Gaussian fits to them are of the same quality as in the case of DLA (see also Ref. 33). As in that case, a quantitative characterization of the spherically averaged properties of the clusters is given by the average deposition radius $\bar{r}_N$ [Eq. (7)], the radius of gyration $R_g(N)$ [Eq. (6)], and the width of the active zone ξ_N [Eq. (8)]. (The center-of-mass motion is considered separately in Sec. IV.) Coarse graining was not carried out in this case. The results are displayed in Figs. 4 and 5.

Since we have generated five times as many clusters as in our previous study of the $d=2$ case, the statistics are good enough for a three-parameter fit in the range $100 < N < 4000$. Least-square fits of $\bar{r}_N$ and $R_g(N)$ to a form $AN^{\nu}+B$ produces the estimates shown in Table II. Since both $\bar{r}_N$ and $R_g(N)$ lead to the expected result $\nu = 1/d = \frac{1}{2}$, one might conclude that, apart from the next to leading constant term B, there are no significant corrections to scaling in the given region of N. This conclusion is further supported by the good accuracy of the estimate of the amplitude A of the leading singularity. Indeed, the space-filling nature of the Eden process implies that $A = 1/\sqrt{\pi} \approx 0.56$ for $\bar{r}_N$ while $A = 1/\sqrt{2\pi} \approx 0.40$ for $R_g(N)$, both numbers agreeing very well with the numerical results (Table I). Although it is quite evident from visual observation that every lattice site is occu-

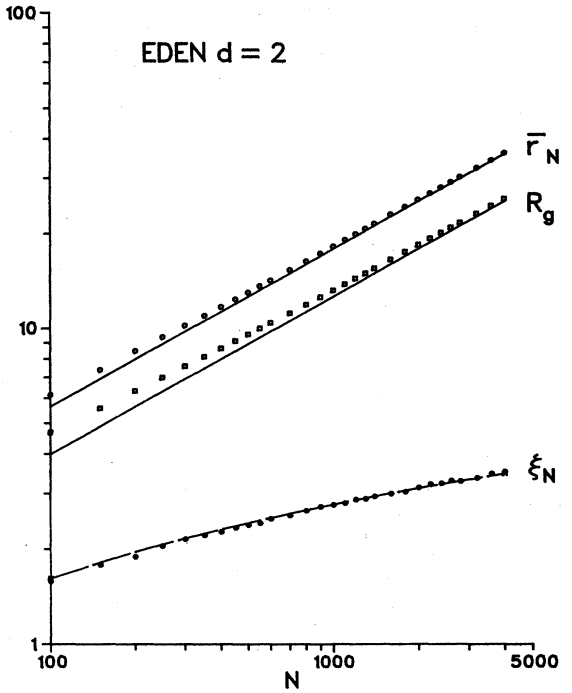

FIG. 4. Mean deposition radius $\bar{r}_N$, radius of gyration $R_g(N)$, and width of the active zone for 20 000 clusters of 4000 particles for the two-dimensional Eden model. The solid curves $\bar{r}_N = (N/\pi)^{1/2}$, $R_g(N) = (N/2\pi)^{1/2}$ correspond to space-filling clusters; the curve $\xi_N = \frac{1}{2}\ln N - 0.69$ corresponds to the conjecture $\xi_N = (1/d)\ln N + B$ for d-dimensional Eden models.

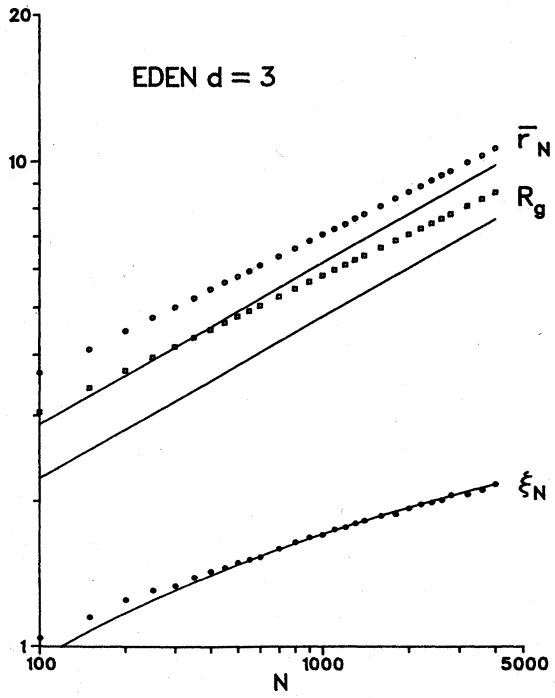

FIG. 5. Plot of $\bar{r}_N$, $R_g(N)$, and ξ_N for the three-dimensional Eden model for 16 000 clusters of 4000 particles. The solid curves $\bar{r}_N = [(3/4\pi)N]^{1/3}$, $R_g(N) = (\frac{3}{5})^{1/2}\bar{r}_N$ are for a space-filling process and $\xi_N = \frac{1}{3}\ln N - 0.59$ corresponds to the conjecture $\xi_N \approx (1/d)\ln N$ for large N.

TABLE II. Parameters in the fit of $\bar{r}_N$ and $R_g(N)$ to the form $AN^{\nu}+B$ in the two- and three-dimensional Eden model. The error bars are of statistical origin, as explained in Sec. II in connection with DLA clusters, and do not include systematic errors due to finite-size effects and due to the restrictive functional form of the fit.

	ν	A	B
$d=2$ $\bar{r}_n$	0.503±0.005	0.55±0.03	0.6±0.2
$R_g(N)$	0.500±0.005	0.40±0.02	0.7±0.1
$d=3$ $\bar{r}_N$	0.31 ±0.03	0.8 ±0.2	0.3±0.6
$R_g(N)$	0.29 ±0.02	0.8 ±0.2	0.2±0.2

pied inside an Eden cluster, we pause here in the numerical analysis to present a simple argument confirming the view that the Eden process leads to complete filling.

Let us start with the assumption that, contrary to what we see, there is a finite density ρ_s of surface sites within a large cluster of N particles. Since the particles are added with equal probability to any surface site in an Eden cluster, the preceding assumption implies that the probability P_i of the $N+1$st particle being deposited in the interior of the cluster is proportional to $\rho_s \bar{r}_N^d$, while the probability P_0 of attaching this particle to the active zone of the cluster can be estimated as $P_0 \sim \bar{r}_N^{d-1}\xi_N$. The active zone is, by definition, the region where the particles are deposited preferentially so we must have $P_i \lesssim P_0$. Since

$$\frac{P_0}{P_i} \sim \frac{1}{\rho_s}\frac{\xi_N}{\bar{r}_N} \sim \frac{1}{\rho_s} N^{\bar{\nu}-\nu} \tag{10}$$

the inequality $P_i \lesssim P_0$ is violated for large N unless $\bar{\nu}=\nu$. This contradiction would constitute a proof of the space-filling nature of the Eden process if the strict inequality $\bar{\nu}<\nu$ could be shown to be valid. Unfortunately, we are able to provide justification for $\bar{\nu}<\nu$ only in the form of numerical data (Figs. 4 and 5) which seem to exclude the possibility that $\bar{\nu}=\nu$. Indeed, fitting the data for ξ_N to a form $AN^{\bar{\nu}}+B$ we obtain $\bar{\nu}=0.04\pm0.02$ and $A=-B=10\pm10$, thus $\bar{\nu}\ll\nu$. In our previous study[34] we used a two-parameter fit $\xi_N \approx \xi_0 N^{\bar{\nu}}$ and obtained $\bar{\nu}=0.18\pm0.03$; thus the improved statistics and the inclusion of the constant term lowered the value of $\bar{\nu}$ indicating the possibility that $\bar{\nu}=0$. Consequently, we tried to analyze the data assuming logarithmic singularity in ξ_N,

$$\xi_N = A(\ln N)^{\sigma}+B \tag{11}$$

and we found an improved χ^2 for $\sigma=1.2\pm0.3$, $A=0.3\pm0.2$, and $B=-0.3\pm0.6$. It is remarkable that if σ is fixed at 1 then the best fit is obtained for $A=0.5$ suggesting that the relationship between the singular parts of ξ_N and $\bar{r}_N$ might be quite simple and of the form

$$\xi_N \approx \ln\bar{r}_N \approx \tfrac{1}{2}\ln N \ . \tag{12}$$

The small value of $\bar{\nu}$ is in agreement with the results of studies[3,31,43] of the number of surface sites N_s. This number can be estimated to scale as

$$N_s \sim \xi_N \bar{r}_N^{d-1} \sim N^{\bar{\nu}+1-1/d} \ , \tag{13}$$

thus, for $d=2$, our calculations yield $N_s \sim N^{0.5}\ln N$ compared to previous reports of $N_s \sim N^{0.5}$ (Refs. 3 and 31) and $N_s \sim N^{0.55}$ (Ref. 43). The only discrepancy is with the estimates of the width of the surface layer through the density profile of the clusters.[31] Clusters of size $N<400$ were studied in Ref. 31 and $\xi_N \sim N^{1/d}$, i.e., $\bar{\nu}=\nu$ was obtained for $d=2$ and 3. We can attribute[34] this discrepancy only to the fact that in the particular way ξ_N is calculated in Ref. 31, it is easy to pick up contributions which are of the order $\bar{r}_N \sim N^{1/d}$.

Apart from decreased accuracy, the results for $d=3$ are quite similar (Fig. 5) to those of the $d=2$ case. As can be seen from Table II, correction to scaling terms other than the constant B are important in the range $100<N<4000$ since $\nu=\frac{1}{3}$ is not obtained with good accuracy and the values of the amplitude A are also off the "space-filling" predictions $A=(3/4\pi)^{1/3}\approx0.62$ for $\bar{r}_N$ and $A=(\frac{3}{5})^{1/2}(3/4\pi)^{1/3}=0.48$ for R_g. It is remarkable, however, that if ν is fixed at $\frac{1}{3}$ then the optimal value of A is close to these predictions for both $\bar{r}_N$ and $R_g(N)$ ($A\simeq0.64$ and $A\simeq0.51$, respectively).

The data for ξ_N can be equally well fit by $\xi_N=AN^{\bar{\nu}}+B$ ($\bar{\nu}=0.07^{+0.07}_{-0.05}$, $A=-B=2.7^{-2.0}_{+8.0}$) or by $\xi_N=A(\ln N)^{\sigma}+B$ ($\sigma=1.4\pm0.5$, $A=0.11^{-0.07}_{+0.40}$, $B=0.1\pm1.0$). The equality $A=-B$ in the power-law fit, however indicates that, as in $d=2$, $\xi_N \sim \ln N$. This indication is further supported by the fact that if one sets $\sigma=1$ in the logarithmic fit, then the best value of A is 0.31 which is close to the value $A=\frac{1}{3}$ expected if the relationship $\xi_N \approx \ln\bar{r}_N$ is valid for any dimension. Hence, on the basis of the $d=2$ and 3 data, one might suspect that the large-N behavior of ξ_N is given by

$$\xi_N \approx \frac{1}{d}\ln N \tag{14}$$

which is a simple enough result to hope that it can be derived analytically.

IV. CENTER-OF-MASS MOTION IN GROWING CLUSTERS

As we have seen in the preceding sections, growing clusters are characterized by quantities like the radius of gyration, the average deposition radius, etc., which are defined with respect to the center of mass of the system. A natural question one might ask is why bother following the motion of the center of mass instead of defining the same quantities with respect to the seed ($N=1$) particle. In this section we try to answer this question by showing that the position of the center of mass fluctuates strongly for clusters of low fractal dimensionality and that these fluctuations might dominate the scaling properties of quantities like the width of the active zone, thus resulting in incorrect exponent estimates. For DLA we also present evidence that the motion of the center of mass is sensitive to the boundary conditions used in actual Monte Carlo simulations.

The importance of separating the center-of-mass motion can be seen in the case of the $d=1$ Eden model which is the $d=1$ version of the DLA as well. A seed particle is placed at the origin and then particles are ran-

domly added on the left or right at the unoccupied lattice sites neighboring the existing cluster. The behavior of the resulting cluster is quite simple and can be calculated exactly. The Nth particle is placed at a distance $N/2$ from the center of mass in units of the lattice constant; thus $\bar{r}_N = N/2$ and we have the obvious result $\nu = 1/d = 1$. Since there are no fluctuations in the deposition radius, $\xi_N = 0$ and consequently $\bar{\nu} = -\infty$, or, if the sharp boundary is interpreted as a surface of width of a lattice constant, then $\xi_N \approx 1$ and $\bar{\nu} = 0$.

We show now that if $\bar{r}_N$ and ξ_N are defined with respect to the seed particle, then the value of $\bar{\nu}$ is altered to $\bar{\nu} = \frac{1}{2}$ reflecting the random walk of the center of mass of the cluster. To do this we calculate probability that the Nth particle is deposited at a distance l $(1 \le l \le N-1)$ from the origin. The calculation consists of enumerating the number of ways $N-2$ particles can be deposited around the origin so that one of the end particles is at a distance $l-1$. This number then has to be multiplied by $2^{-(N-2)}$ because every configuration is equiprobable. The result is the binomial distribution

$$P(l,N) = \frac{(N-2)!}{(l-1)!(N-1-l)!}\left(\tfrac{1}{2}\right)^{N-2} \tag{15}$$

which in the large-l and -N limit becomes the Gaussian distribution

$$P(l,N) \approx \frac{1}{\sqrt{2\pi}\xi_N} e^{-(l-\bar{r}_N)^2/2\xi_N^2} \tag{16}$$

with $\bar{r}_N = N/2$ and $\xi_N = \sqrt{N/2}$ implying $\nu = 1$ as before but $\bar{\nu} = \frac{1}{2}$, different from the previous result. It is clear that the divergence of ξ_N is entirely an artifact due to the uncertainty of the center of mass of the cluster. Indeed the change in the center of mass in the Nth step of the process is

$$x_c(N) - x_c(N-1) = \Delta x_c(N) = \frac{1}{N}[x_N - x_c(N-1)] , \tag{17}$$

where x_N is the coordinate of the Nth particle while $x_c(N)$ is the coordinate of the center of mass after N particles have been deposited. Since $x_N - x_c(N-1) = \pm\frac{1}{2}$, we have $\Delta x_c(N) = \pm\frac{1}{2}$, i.e., the center of mass executes a random motion with step size $\frac{1}{2}$. So, after N steps the uncertainty of its position is $\sqrt{N/2}$ which is just ξ_N as obtained previously.

It is clear now that the separation of the center-of-mass motion in $d = 1$ is essential in revealing the true nature of the surface of the cluster. In order to have an idea about the situation in higher dimensions we shall estimate the uncertainty of the center of mass assuming that its motion is a random walk but the step size is changing as the cluster is built. Let $\mathbf{r}_c(N) = \sum_{i=1}^{N} \mathbf{r}_i / N$ be the position of the center of mass after N particles have been deposited where $\mathbf{r}_i$ is the position of the ith particle. The change of $\mathbf{r}_c$ when the Nth particle is added can be written as

$$\mathbf{r}_c(N) - \mathbf{r}_c(N-1) = \Delta\mathbf{r}_c(N) = \frac{1}{N}[\mathbf{r}_N - \mathbf{r}_c(N-1)] . \tag{18}$$

The average magnitude of this vector is estimated to be

$$\langle\, |\Delta\mathbf{r}_c(N)|\, \rangle_{\text{av}} \approx \frac{1}{N}\bar{r}_N \sim N^{1/D-1} , \tag{19}$$

where used the fact that $|\mathbf{r}_N - \mathbf{r}_c(N-1)|$ is the deposition radius of the Nth particle. Since $\mathbf{r}_c(N)$ can be written as

$$\mathbf{r}_c(N) = \sum_{i=1}^{N} \Delta\mathbf{r}_c(i) \tag{20}$$

and since we assume

$$\langle \Delta\mathbf{r}_c(i)\Delta\mathbf{r}_c(j)\rangle_{\text{av}} = \langle[\Delta\mathbf{r}_c(i)]^2\rangle_{\text{av}}\delta_{ij} , \tag{21}$$

we obtain

$$\langle \mathbf{r}_c^2(N)\rangle_{\text{av}} = \sum_{i=1}^{N} \langle[\Delta r_c(i)]^2\rangle_{\text{av}} \sim \sum_{i=1}^{N} i^{2/D-2} \sim N^{2/D-1} . \tag{22}$$

Hence the magnitude of $\mathbf{r}_c(N)$ scales as

$$r_c(N) = \langle \mathbf{r}_c^2(N)\rangle_{\text{av}}^{1/2} \sim N^{(2-D)/2D} . \tag{23}$$

It follows from this formula that the uncertainty in the position of the center of mass becomes unbounded in the limit $N \to \infty$ if $D < 2$. This result is in agreement with the general expectation that the long wavelength fluctuations are more important in low-dimensional systems. It also follows from Eq. (22) that if $\bar{\nu} < (2-D)/2D$ then correct estimates of $\bar{\nu}$ can be obtained only after the separation of the center-of-mass motion.

For the Eden model, Eq. (23) predicts $r_c(N) \sim N^{1/2}$, $r_c(N) \sim N^0$ (logarithmic singularity), and $r_c(N) \sim \text{const} + aN^{-1/6}$ for $d = 1,2,3$, respectively. The result for $d = 1$

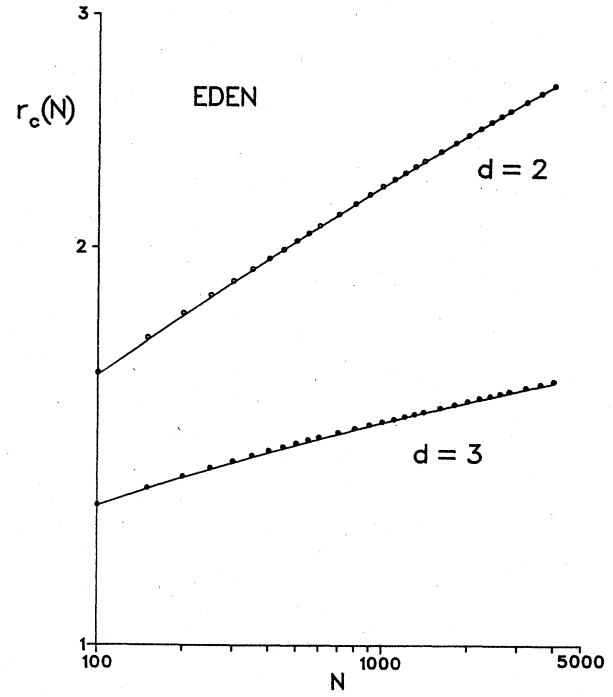

FIG. 6. Displacement of the center of mass $r_c(N)$ for two- and three-dimensional Eden models. The solid curves are $r_c(N) = 0.075(\ln N)^{3/2} + 0.86$ for $d = 2$, and $r_c(N) = 0.29(\ln N)^{0.6} + 0.55$ for $d = 3$.

agrees with the exact calculation and the $d=2$ Monte Carlo data (Fig. 6) are also best fit by the expected functional form $r_c(N)=A\ln^{\sigma}N+B$ with $\sigma=1.5\pm0.1$, $A=0.89\pm0.05$, and $B=0.07\pm0.02$. It is harder to analyze the $d=3$ data (Fig. 6) since the predicted exponent $-\frac{1}{6}$ comes from the next to leading term and also because this exponent is small. Actually, the best fit is again obtained by assuming a logarithmic singularity [Eq. (10)] with $\sigma=0.6\pm0.2$, $A=0.3\pm0.2$, and $B=0.5\pm0.3$. Fits of similar quality can be obtained, however, by using the form $r_c(N)\sim\text{const}+aN^{\sigma}$ with $-0.1<\sigma<-0.03$. We believe that in $d=3$, the range of N ($100<N<4000$) is too small and the fluctuations in the data points are too large for a full three-parameter fit in order to extract the next to leading term.

In the case of DLA, Eq. (23) predicts $r_c(N)\sim N^{0.1}$ ($d=2$) and $r_c(N)\sim\text{const}+aN^{-0.1}$ ($d=3$). Thus the motion of the center of mass does not seem to be an important matter since, as our Monte Carlo simulation indicates, $\xi_N\sim N^{0.5}$ in $d=2$ and $\xi_N\sim N^{0.3}$ in $d=3$. There is, however, another effect resulting from the particular way the Monte Carlo simulations are executed which make the examination of $\mathbf{r}_c(N)$ relevant. One of the problems with the computer simulations of DLA is that the particle launched at a distance R_i from the seed particle sometimes wanders so far away that it is impractical to wait until it returns. Instead, the particle is destroyed if its distance from the seed particle becomes greater than R_0 and a new particle is launched at a distance R_i. In actual calculations, R_i is usually taken to be somewhat larger than the radius of the cluster; thus R_i varies as the cluster grows, but $R_0/R_i=\alpha$ is kept constant. As we shall show below, the scaling behavior of $r_c(N)$ is critically dependent on this ratio $\alpha=R_0/R_i$.

In order to understand the physical basis for this dependence, we remember that in DLA one actually solves the problem of crystal growth into a supercooled liquid under the condition that the surface tension of the crystal is zero.[2] Mathematically this means that one solves the Laplace equation for the appropriately scaled temperature field u:

$$\Delta u=0 \tag{24}$$

with the boundary conditions (AG denotes aggregate surface)

$$u_{\mathrm{AG}}=u_0,\quad u(r=\infty)=0\ ,$$

where u_0 is proportional to the degree of supercooling at $r=\infty$. Having solved this problem, the relative probability of growth at different surface sites is obtained from the ratio of $|\nabla u|$ at those sites. Now, the simulation procedure that the particle is thrown away if $r>R_0$ corresponds to the boundary condition $u(r=R_0)=0$ instead of $u(r=\infty)=0$. Thus crystal growth takes place in a spherical container instead of the infinite medium. As a result, the center-of-mass coordinate ceases to be a marginal variable. Once fluctuations move the center of mass off the origin, the crystal will grow preferentially in the direction of the displacement since the walls are closer and consequently the temperature gradient is larger in that direction. To have a quantitative estimate of the effect of walls at finite distance, we shall consider the $d=1$ case which can be solved exactly even in the case when the walls are moved as is done in Monte Carlo simulations.

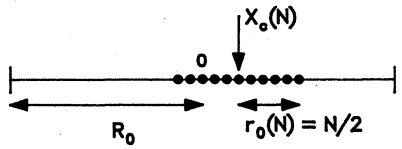

FIG. 7. Small one-dimensional DLA or Eden cluster with center of mass at $x_c(N)$ and seed at $x=0$. The discard distance $R_0=2(x_c+r_0)$ in this case.

The solution of the Laplace equation in $d=1$ is $u=px+q$. The constants p and q are determined from the boundary conditions $u(\pm R_0)=0$, $u(x_c\pm r_0)=u_0$ (see Fig. 7). From these conditions one obtains $p_+=u_0/(x_c+r_0-R_0)$ for the region $x_c+r_0<x<R_0$ while $p_-=u_0/(x_c+r_0-R_0)$ for $-R_0<x<x_c-r_0$. Since the probability of growth is proportional to $|\nabla u|=|p_{\pm}|$ we have for the probability $P_{\pm}$ of the cluster growing in the + or − direction

$$P_{\pm}=\tfrac{1}{2}\pm\frac{x_c}{2(R_0-r_0)}\ . \tag{25}$$

If a particle is added on the right- or left-hand side of the cluster then the change of x_c is given by

$$x_c(N+1)-x_c(N)=\pm\frac{r_0(N)+1}{N+1}\ , \tag{26}$$

and so the average shift of x_c can be expressed as

$$\begin{aligned}\delta x_c(N)&=(P_+-P_-)\frac{r_0(N)+1}{N+1}\\&=\frac{x_c(N)[r_0(N)+1]}{(N+1)[R_0-r_0(N)]}\ .\end{aligned} \tag{27}$$

Thus if we use the fact that $R_0=\alpha R_i=\tilde{\alpha}r_0(N)$ then in the large N limit we obtain

$$\frac{\delta x_c(N)}{x_c(N)}\approx\frac{1}{(\tilde{\alpha}-1)N}\ , \tag{28}$$

yielding

$$x_c(N)\sim N^{1/(\tilde{\alpha}-1)}\ . \tag{29}$$

Actually, since R_i is usually taken to be $\approx r_0(N)$, $\tilde{\alpha}=\alpha$ and the ratio R_0/R_i determines the scaling of $x_c(N)$. We believe this feature to be pertinent to higher dimensions as well. In Fig. 8 we display $r_c(N)$ for the $d=2$ and 3 case and can definitely see the effect of varying α, the general trend being that the scaling exponent of $r_c(N)$ decreases as α is increased and in general $r_c(N)$ is smaller for larger α reflecting the fact that the "effective force" acting on the center of mass is smaller if the walls are farther away.

V. CONCLUSION

We have studied, in this article, the surface properties of growing clusters in two distinct growth models, the Eden model and diffusion-limited aggregation. For DLA

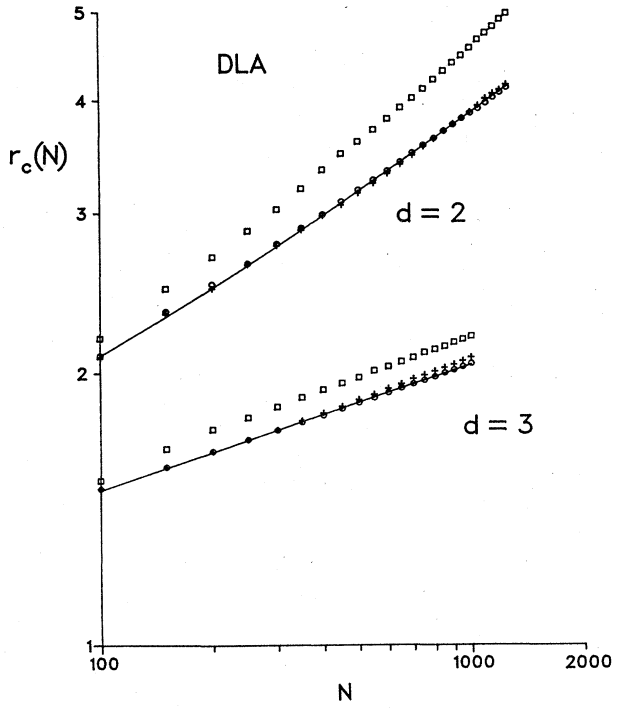

FIG. 8. Displacement of the center of mass $r_c(N)$ as a function of N for DLA in $d=2$ and 3. The points are for fixed $l_0=8$ in both cases. For $d=2$ the squares are the results for $\alpha=2$, the crosses for $\alpha=3$, and the circles for $\alpha=4$. In $d=3$ the squares correspond to $\alpha=2$, the crosses to $\alpha=3$, and the circles to $\alpha=5$. The solid curve in $d=2$ is the line $r_c(N)=0.758+0.242N^{0.370}$ while in $d=3$ it is $r_c(N)=-0.158+0.915N^{0.127}$.

we have documented the existence of a second diverging length scale $\xi_N \sim N^{\bar{\nu}}$ with $\bar{\nu} < \nu = 1/D$ for $d=2$ and 3, distinct from the length $\bar{r}_N$ which characterizes the size of the cluster. In the Eden process the width of the surface layer also diverges $\xi_N \sim (\ln N)^{\sigma}$ and our simulations indicate that the correct functional form may be $\xi_N \sim (1/d)\ln N$. Both of these results should be investigated further by studying larger clusters and, in the case of DLA, by varying the growth parameters α and l_0.

We have also found that in both models $P(r,N)$ is extremely well represented by a Gaussian function (1). This immediately suggests the possibility of inverting the present approach. Instead of generating clusters and calculating $P(r,N)$ one can postulate Eq. (1) and simulate growth through this probability density. One then has the freedom to choose $\bar{\nu}$, as well as the other parameters which determine ξ_N. In this way it may be possible to identify the way the properties of the frozen structure are affected by the scaling properties of the surface layer.

Finally, we mention that some of the other models which have been extensively studied in recent years may have striking surface properties. In particular the tip-priority model[11] seems to give rise to a surface layer which varies as the tip-priority factor is changed. It would be interesting to investigate whether the exponent $\bar{\nu}$ in this case varies continuously as a function of the priority factor or whether there are competing fixed points and the apparent continuous variation[11] is merely a manifestation of a type of crossover phenomenon familiar from equilibrium critical phenomena.

ACKNOWLEDGMENT

This research was supported by the Natural Sciences and Engineering Research Council of Canada.

*On leave from the Institute for Theoretical Physics, Eötvös University, H-1088 Budapest, Hungary.
[1]*Kinetics of Aggregation and Gelation* edited by F. Family and D. P. Landau (North-Holland, Amsterdam, 1984).
[2]T. A. Witten and L. M. Sander, Phys. Rev. Lett. **47**, 1400 (1981).
[3]M. Eden, *Proceedings of the Fourth Berkeley Symposium on Mathematical Statistics and Probability,* edited by F. Neyman (University of California, Berkeley, 1961), Vol. IV, p. 223.
[4]P. Meakin, Phys. Rev. Lett. **51**, 1119 (1983).
[5]M. Kolb, R. Botet, and R. Jullien, Phys. Rev. Lett. **51**, 1123 (1983).
[6]S. R. Forrest and T. A. Witten, J. Phys. A **12**, L109 (1979).
[7]D. A. Weitz and M. Oliveria, Phys. Rev. Lett. **52**, 1433 (1984).
[8]L. Niemeyer, L. Pietronero, and H. J. Wiesmann, Phys. Rev. Lett. **52**, 1033 (1984).
[9]L. Paterson, Phys. Rev. Lett. **52**, 1621 (1984).
[10]P. A. Rikvold, Phys. Rev. A **26**, 647 (1982).
[11]Y. Sawada, S. Ohta, M. Yamazaki, and H. Honjo, Phys. Rev. A **26**, 3557 (1982).
[12]J. S. Langer, Rev. Mod. Phys. **52**, 1 (1980).
[13]P. Meakin, Phys. Rev. A **27**, 2616 (1983).
[14]P. Meakin, Phys. Rev. A **29**, 997 (1984).
[15]P. Meakin, Phys. Rev. B **29**, 3722 (1984).
[16]D. Wilkinson and J. Willemsen, J. Phys. A **16**, 3365 (1983).
[17]D. Wilkinson and M. Barsony, J. Phys. A **17**, L129 (1984).
[18]M. T. Vold, J. Colloid Sci. **18**, 684 (1963).
[19]D. N. Sutherland, J. Colloid Sci. **22**, 300 (1966), **25**, 373 (1967).
[20]D. Bensimon, E. Domany, and A. Aharony, Phys. Rev. Lett. **51**, 1394 (1983).
[21]D. Bensimon, B. Shraiman, and S. Liang, Phys. Lett. A **102**, 238 (1984).
[22]M. Muthukumar, Phys. Rev. Lett. **50**, 839 (1983).
[23]M. Tokuyama and K. Kawasaki, Phys. Lett. A **100**, 337 (1984).
[24]H. Hentschel, Phys. Rev. Lett. **52**, 212 (1984).
[25]M. Nauenberg, Phys. Rev. B **28**, 449 (1983).
[26]R. Ball, M. Nauenberg, and T. A. Witten, Phys. Rev. A **29**, 2017 (1984).
[27]H. Gould, F. Family, and H. E. Stanley, Phys. Rev. Lett. **50**, 686 (1983).
[28]P. Meakin and T. A. Witten, Phys. Rev. A **28**, 2985 (1983).
[29]P. Meakin Phys. Rev. B **30**, 4207 (1984).
[30]L. Sander in Ref. 1.
[31]H. P. Peters, D. Stauffer, H. P. Hölters, and K. Loewenich, Z. Phys. B **34**, 399 (1979).
[32]D. Stauffer, Phys. Rep. **54**, 1 (1979).
[33]M. Plischke and Z. Rácz in Ref. 1.
[34]M. Plischke and Z. Rácz, Phys. Rev. Lett. **53**, 415 (1984).
[35]K. Binder, Ann. Phys. (N.Y.) **98**, 390 (1976).
[36]P. Meakin, Phys. Rev. A **27**, 604 (1983).

[37]P. Meakin, Phys. Rev. A **27**, 1495 (1983).
[38]P. Meakin and J. M. Deutch, J. Chem. Phys. **80**, 2115 (1984).
[39]Z. Rácz and T. Vicsek, Phys. Rev. Lett. **51**, 2382 (1983).
[40]L. Sander, Z. M. Cheng, and R. Richter, Phys. Rev. B **28**, 6394 (1983).
[41]L. Turban and J. Debierre, J. Phys. A **17**, L289 (1984).
[42]W. Feller, *An Introduction to Probability Theory and its Applications* (Wiley, New York, 1970), Vol. 1, Chap. 14.
[43]T. Williams and R. Bjerknes, Nature **236**, 19 (1972).
[44]P. Tautu, Z. Krebsforsch. **91**, 223 (1978).
[45]P. Meakin (unpublished).